# Apoptosis is an obstacle to the differentiation of adipose-derived stromal cells into astrocytes

Xiaodong Yuan[1], Qiaoyu Sun[1], Ya Ou[1], Shujuan Wang[1], Wenli Zhang[2], Hongliang Deng[1], Xiaoying Wu[1], Lili Zhang[1]

1 Department of Neurology, Kailuan General Hospital, Hebei United University, Tangshan, Hebei Province, China
2 Department of Electron Microscopy, Hebei United University, Tangshan, Hebei Province, China

*Corresponding author:*
*Xiaodong Yuan, Department of Neurology, Kailuan General Hospital, Hebei United University, Tangshan 063000, Hebei Province, China, yxd68@sohu.com.*

## Abstract

Previous studies have demonstrated that nerve cells differentiated from adipose-derived stromal cells after chemical induction have reduced viability; however, the underlying mechanisms remained unclear. In this study, we induced the differentiation of adult adipose-derived stromal cells into astrocytes using chemical induction. 3-(4,5-Dimethylthiazol-2-yl)-2,5-diphenyltetrazolium bromide assay and flow cytometry showed that, with increasing induction time, the apoptotic rate gradually increased, and the number of living cells gradually decreased. Immunohistochemical staining demonstrated that the number of glial fibrillary acidic protein-, caspase-3- and caspase-9-positive cells gradually increased with increasing induction time. Transmission electron microscopy revealed typical signs of apoptosis after differentiation. Taken together, our results indicate that caspase-dependent apoptosis is an obstacle to the differentiation of adipose-derived stromal cells into astrocytes. Inhibiting apoptosis may be an important strategy for increasing the efficiency of induction.

*Key Words: nerve regeneration; adult adipose-derived stromal cells; cell apoptosis; caspase-dependent apoptosis; cell differentiation; astrocytes; caspase-9; caspase-3; neural regeneration*

## Introduction

Adipose-derived stromal cells are stem cells with multi-directional differentiation potential, and have numerous advantages, including strong proliferative ability, low immunogenicity and no legal or ethical issues (Zuk et al., 2001, 2002; McIntosh et al., 2006; Liu et al., 2007; Wu et al., 2013; Cao et al., 2014). Previous studies have shown that adult adipose-derived stromal cells can be successfully transformed into neurons and astrocytes (Safford et al., 2002; Ashjian et al., 2003; Yoshimura et al., 2007; Liu et al., 2010; Ye et al., 2010; Ou et al., 2011a, b). Astrocytes participate in various physiological process and brain development, and help maintain a stable environment for neurons. They also play a very important role in repair and regeneration after brain injury and neurodegeneration (Pekny and Nilsson, 2005; Jacobsen et al., 2006; Di Giorgio et al., 2007; Holden, 2007; Van Den Bosch and Robberecht, 2008). The *in vitro* induction of these astroglia has provided a new way for the treatment of clinical nervous system damage and neurodegenerative disorder (Kang et al., 2003; Goldman, 2005; Nakagami et al., 2006). However, when 3-isobutyl-1-methylxanthine was used to induce adipose-derived stromal cell differentiation, the survival time of the resulting astrocytes was only approximately 30 days (Liu et al., 2010; Ou et al., 2011b), limiting further research and clinical applications.

Our previous experiments showed that apoptosis is a major cause of death of neurons originating from adipose-derived stromal cells (Cai et al., 2011; Lu et al., 2012). Studies have shown that there are two types of apoptosis; caspase-dependent and caspase-independent (Daniel, 2000; Vittar et al., 2010; Zhang et al., 2011). In caspase-dependent apoptosis, the caspase family of proteases mediates apoptosis (Gil and Esteban, 2000; Chen and Wang, 2002; Kavitha et al., 2012). The caspases include two types of caspases (Ren et al., 2012; Tatsuta et al., 2013); initiators, such as caspase-9, which cleave and activate other caspases (von Roretz et al., 2013), and effectors, such as caspase-3, which cleave various substrates and decompose cell structure or inactivate enzymes (Kang et al., 2010; Wirawan et al., 2010). As an "executioner" protease, caspase-3 plays an important role in apoptosis (Compton and Cidlowski, 1986; Adrain et al., 2001; Slee et al., 2001). Previous studies have shown that caspase-dependent apoptosis occurs during adipose-derived stromal cell differentiation into neurons (Lu et al., 2012). Therefore, in this study, we investigated caspase-dependent apoptosis during adipose-derived stromal cell differentiation into astrocytes.

## Materials and Methods

### Extraction and culture of adult adipose-derived stromal cells

Volunteers were 13 healthy adults, aged 20–35 years, from the Physical Check-up Center, Kailuan General Hospital, Tangshan, Hebei Province, China. Needle aspiration was
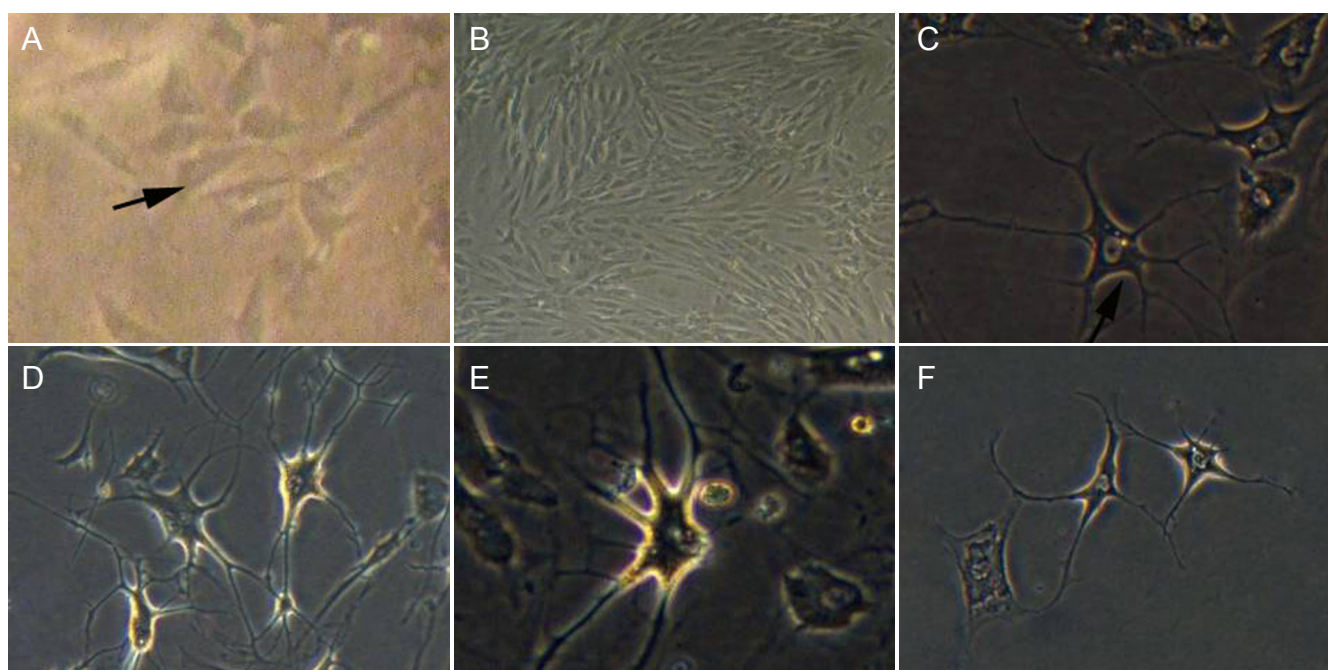
**Figure 1 Changes in cell morphology before and after ADSC induction (inverted phase contrast microscope).**
(A) Primary ADSCs cultured for 24 hours. Cells (arrow) are triangular (× 100). (B) ADSCs at the third passage at 7 days. Cells were fusiform and formed a whorl pattern (× 40). (C) At 48 hours, cell bodies of ADSCs (arrow) were polygonal, with a surrounding halo. The nucleus was large and oval-shaped, and slender protrusions with many branches extended out (× 100). (D) At 7 days, refractivity of cell bodies was further enhanced, and there were many slender protrusions around cell bodies, forming a meshwork (× 100). (E) At 14 days, cell morphology showed no significant changes compared with 7 days (× 100). (F) At 21 days, cell processes became shorter and fewer (× 100). ADSCs: Adipose-derived stromal cells.
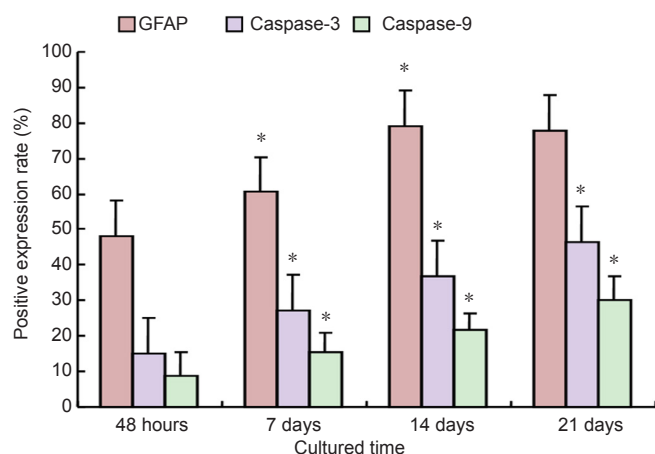


**Figure 3 Positive expression rate of glial fibrillary acidic protein (GFAP), caspase-3 and caspase-9 in adult adipose-derived stromal cells differentiated at different time points (immunocytochemistry).**
Data were expressed as mean ± SD. Differences were compared using one-way analysis of variance followed by Student-Newman-Keuls test. Experiments were repeated in triplicate. ∗$P < 0.05$, *vs.* previous time point.
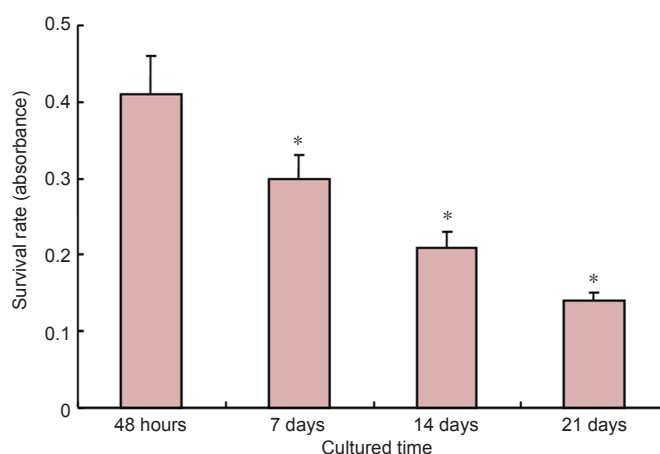


**Figure 4 Survival rate of adult adipose-derived stromal cells differentiated at different time points assessed with MTT.**
Data were expressed as mean ± SD. Differences were compared using one-way analysis of variance followed by Student-Newman-Keuls test. Experiments repeated in triplicate. ∗$P < 0.05$, *vs.* previous time point. MTT: 3-[4, 5-Dimethylthiazol-2-yl]-2,5-diphenyl tetrazolium bromide.

used to extract abdominal subcutaneous adipose tissue of adult volunteers without endocrine or hematological diseases. 10–30 mL adipose tissue was collected each time. Written informed consent from the volunteers was obtained. The protocol was approved by the Medical Ethics Committee of Kailuan General Hospital of Hebei United University, China.

Based on the method of Ye et al. (2010) and other exper-

imental protocols, 0.1% collagenase type I (Solarbio, Beijing, China) was added, and the tissue was placed in a 37°C water bath for digestion for 1 hour and then centrifuged at 1,000 r/min for 5 minutes. Supernatant was aspirated out. The undigested tissues and the underlying cells were stirred to mix, and then filtered through a 100-mesh sieve. The samples were centrifuged at 1,000 r/min for 5 minutes, and the
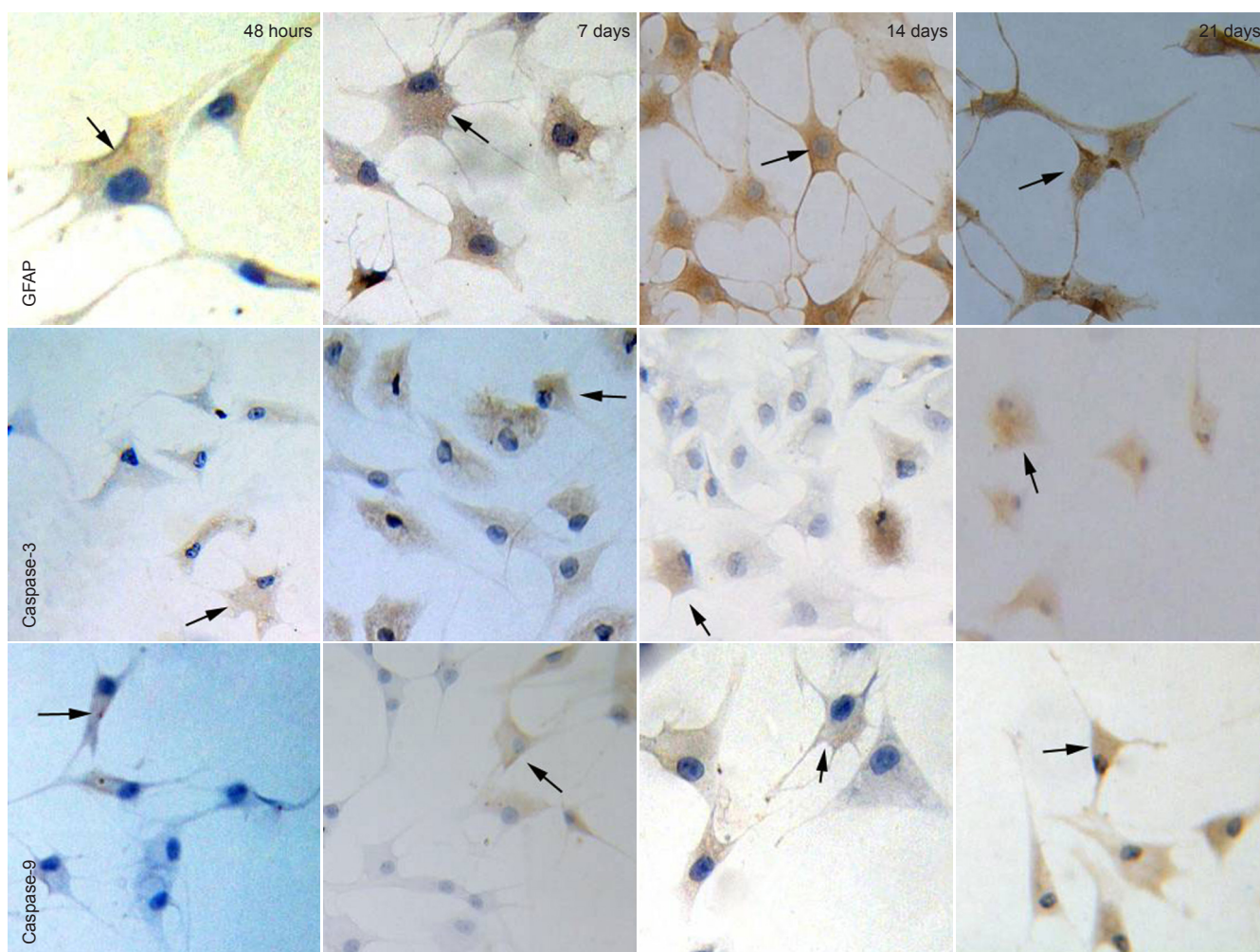
**Figure 2 Expression of GFAP, caspase-3 and caspase-9 at various time points after adipose-derived stromal cells differentiation (immunocytochemical staining, inverted phase contrast microscope, × 200).**
Arrows indicate GFAP-, caspase-3- and caspase-9-positive cells. GFAP: Glial fibrillary acidic protein.

supernatant was removed. The remaining cell pellet was seeded into culture flasks at a density of $8 \times 10^3/cm^2$ and placed in a 37°C, 5% $CO_2$ humidified incubator. The culture medium was replaced after 48 hours to remove residual erythrocytes and non-adherent impurities. The culture medium was replaced every 2–3 days. About 10–14 days after the cells reached 90% confluence, trypsin-ethylenediaminetetraacetic acid was used for digestion, and cells were passaged at a 1:2 ratio. Morphological changes in cells were observed using an inverted phase contrast microscope (Olympus, Tokyo, Japan).

### Adult adipose-derived stromal cell differentiation into astrocytes

Passage 3–6 adipose-derived stromal cells, in good condition, were digested with trypsin-ethylenediaminetetraacetic acid and slides were prepared. When the cells reached 70–80% confluence, the medium was removed, inducer was added, and morphological changes were observed after 48 hours and 7, 14 and 21 days under the inverted phase contrast microscope. Inducer components: 0.5 mmol/L 3-isobutyl-1-methylxanthine (Sigma, St. Louis, MO, USA), 1 μmol/L dexamethasone, 10 μmol/L insulin, 200 μmol/L indometh-

acin, 10 mmol/L hydroxyethyl piperazine ethanesulfonic acid (Hyclone, Logan, UT, USA), 2 mmol/L glutamine, 1% non-essential amino acids, 0.5% absolute ethyl alcohol, 10% fetal bovine serum (Hyclone), 100 U/mL penicillin and 100 μg/mL streptomycin, and 85% high-glucose Dulbecco's modified Eagle's medium (DMEM) (Hyclone).

### Glial fibrillary acidic protein, caspase-3 and caspase-9 expression in the induced cells

At 48 hours, and 7, 14 and 21 days after induction, cells were fixed in 4% paraformaldehyde for 30 minutes, permeabilized using 0.1% TritonX-100 for 8 minutes, and incubated with 3% $H_2O_2$ for 10 minutes. Cells were then incubated in working solutions of primary antibodies–rabbit anti-human glial fibrillary acidic protein (1:100; Beijing Biosynthesis Biotechnology, Beijing, China), caspase-9 (1:100; Beijing Biosynthesis Biotechnology) and rabbit anti-human caspase-3 monoclonal (1:100; Boster, Wuhan, Hubei Province, China) at 4°C overnight, and then with goat anti-rabbit IgG-horseradish peroxidase (1:50; Beijing Zhongshan Goldbridge, Beijing, China) for 30 minutes at 37°C. Labeling was visualized with 3,3′-diaminobenzidine (Beijing Zhongshan Golden Bridge

Biotechnology), and cells were then stained with hematoxylin. Immunoreactive cells were counted at high magnification (× 100). Five fields were quantified per sample. Three samples in each group were observed under the inverted phase contrast microscope.

### 3-(4,5-Dimethylthiazol-2-yl)-2,5-diphenyltetrazolium bromide (MTT) assay for cell viability after induction

Adipose-derived stromal cells at passages 3–6 were digested and seeded onto 12-well culture plates, and inoculated at a density of $1 \times 10^5$ cells/well. At 48 hours, and 7, 14 and 21 days after induction, cells in each well were incubated with 5 mg/mL MTT (Sigma), 100 μL, at 37°C for 4 hours. The liquid in the well was discarded, and 1,000 μL dimethyl sulfoxide was added to each well. The plates were then agitated at a low speed of 1,000 r/min for 15 minutes. 100 μL aliquots of the solutions were transferred to a 96-well plate and the absorbance at 490 nm was measured using a microplate reader (Thermo Scientific, Pittsburgh, PA, USA). The absorbance is directly proportional to the number of living cells (Wyllie, 1980). Each experiment was repeated five times.

### Quantification of early apoptotic cells by flow cytometry

The cells induced for 48 hours, and 7, 14 and 21 days were digested and collected. A single cell suspension was prepared at a concentration of $1 \times 10^6$/mL and centrifuged at 1,000 r/min for 5 minutes. The supernatant was discarded, and then 190 μL buffer (Invitrogen, Carlsbad, CA, USA) and 10 μL PI dye solution (Invitrogen) were added. The samples were protected from light and quantified by flow cytometry (BD FACS-Calibur, San Jose, CA, USA) within 1 hour. Each experiment was repeated three times.

### Ultrastructural characteristics of astrocytes and apoptotic cells after induction

The cells induced for 14 days were digested, centrifuged, and fixed in 3% glutaraldehyde and 1% osmic acid, followed by propionaldehyde dehydration and epoxy resin embedding. Cells were sliced using a microtome (Abnova, Walnut, CA, USA) and stained with 2% uranyl acetate and lead citrate. The ultrastructure of cells was observed and photographed with a transmission electron microscope (H7650, Hitachi, Tokyo, Japan).

### Statistical analysis

All experimental data were analyzed using SPSS 13.0 (SPSS, Chicago, IL, USA). Measurement data were expressed as mean ± SD. Intragroup differences were compared using one-way analysis of variance followed by Student-Newman-Keuls test. Values of $P < 0.05$ were considered statistically significant.

## Results

### Morphological changes in cells differentiated from adipose-derived stromal cells

Primary cultured adipose-derived stromal cells adhered at 24 hours, and were observed under the inverted phase contrast microscope. Cells had a triangular and short fusiform appearance (Figure 1A). After 48 hours of culture, the cells had a long fusiform shape, similar to that of the fibroblasts. At 7–10 days, a large number of long spindle-shaped cells were arranged in a whorl pattern (Figure 1B). When passaged to the third generation, adipose-derived stromal cells were almost fusiform. At 24 hours after induction, the cytoplasm retracted to the nucleus (Figure 1C). At 48 hours after induction, round, polygonal or irregular-shaped cells were surrounded by a halo. Parts of cell bodies stretched out slender processes and multiple branches. The cytoplasm was uniform, the nucleus was oval or round, and nucleoli were visible. At 7 days after induction, some of the cells showed the shape of typical astrocytes. Simultaneously, cell protrusions were more extensive, slender branches increased in number and displayed a reticular appearance. The cytoplasm was uniform, the nucleus was large, oval or round, and more biased towards one side of the cell body. Nucleoli were clearly visible (Figure 1D). At 14 days after induction (Figure 1E), cell morphology showed no significant changes from that at 7 days. At 21 days after induction, the number of cells was significantly reduced (Figure 1F). Cells were triangular or irregularly shaped, and cell protrusions were shorter and less numerous than at 14 days of induction. The nucleus showed no significant changes compared with day 14.

### Expression of glial fibrillary acidic protein, caspase-3 and caspase-9 during adipose-derived stromal cell differentiation

At 48 hours of induction, glial fibrillary acidic protein expression was observed in a part of the cytoplasm by immunocytochemical staining. The number of glial fibrillary acidic protein-positive cells gradually increased ($P < 0.05$), and peaked at 14 days. At 21 days, there was no significant difference in the number of glial fibrillary acidic protein-positive cells compared with 14 days ($P > 0.05$). Expression of caspase-3 and caspase-9 was mainly observed in the cytoplasm. The number of caspase-3- and caspase-9-positive cells gradually increased over the induction period ($P < 0.05$; Figures 2, 3).

### Cell survival after adult adipose-derived stromal cell differentiation

MTT assay showed that the survival rate of cells gradually decreased over time: at 48 hours, and 7, 14 and 21 days of induction ($P < 0.05$; Figure 4).

### Early apoptosis after adult adipose-derived stromal cell differentiation

Flow cytometry revealed that at 48 hours, and 7, 14 and 21 days after induction, the apoptotic rate was 4.43 ± 0.26%, 7.80 ± 0.53%, 11.93 ± 0.34% and 14.72 ± 0.43%, respectively. The apoptotic rate gradually increased over time: at 48 hours, and 7, 14 and 21 days ($P < 0.05$; Figure 5).

### Apoptosis and ultrastructural features of astrocytes differentiated from adipose-derived stromal cells

Under the transmission electron microscope, at 14 days after differentiation, the cell bodies of astrocytes were round

or oval. The membrane surface was not smooth, and there were numerous processes. There were varying amounts of bundles of fibers, endoplasmic reticulum, lysosomes and mitochondria in the cytoplasm. Mitochondrial volume was large, and nuclei were oval or irregularly shaped, having 1 or 2 nucleoli, more euchromatin, and reduced and dispersed heterochromatin. The cell bodies of apoptotic astrocytes narrowed, processes from the cell membrane were noticeably decreased or missing, and the surface was smooth. In the cytoplasm, mitochondria exhibited swelling, volume was increased, and the cristae were ruptured and vacuolated. Nuclei were irregular; the nuclear membranes were wrinkled and retracted or even showed karyolysis. Chromatin was reduced, but the amount of heterochromatin was increased. The nuclear chromatin was condensed, and often accumulated near the edges of the nuclear membrane, with blocky or crescent-shaped bodies (Figure 6).

## Discussion

Numerous studies have shown that adipose-derived stromal cells can successfully differentiate into astrocytes *in vitro* (Safford et al., 2002; Ashjian et al., 2003; Liu et al., 2010; Ou et al., 2011b). The induced cells have the typical morphology of astrocytes and express specific markers, and have a characteristic ultrastructure and electrophysiological properties (Ou et al., 2011a). However, our previous experiments showed that many cells died during adipose-derived stromal cell differentiation, and the number of viable cells decreased with increasing length of induction (Liu et al., 2010; Ou et al., 2011b), thereby limiting further research and hindering the application of astrocytes differentiated from adipose-derived stromal cells. Indeed, in the present study, although the expression rate of glial fibrillary acidic protein, the specific marker of astrocytes, reached a peak of 79.2% at 14 days, the number of viable cells had decreased. Therefore, it is necessary to perform further research on the mechanisms of cell death during the differentiation of adipose-derived stromal cells into astrocytes, and to optimize cell differentiation protocols to improve the survival rate of astrocytes differentiated from adipose-derived stromal cells.

Apoptosis is a process of programmed cell death (Wyllie, 1980; Johansson et al., 2010; Giansanti et al., 2011; Freire, 2012; Igder et al., 2013; Tognon et al., 2013). Our previous studies showed that apoptosis is a major cause of the death of neurons differentiated from adipose-derived stromal cells (Cai et al., 2011; Lu et al., 2012). As the preferred method for early detection of apoptotic cells, Annexin V/PI double-staining and flow cytometry can be used to analyze early apoptotic cells efficiently (Nicoletti et al., 1991; Grebeňová et al., 2004; Samsel et al., 2004; Suárez et al., 2004; Guo et al., 2011; Wlodkowic et al., 2013). Therefore, we studied cell death rate in the early stage by flow cytometry. The results demonstrated that the death rate increased over time, peaking at 21 days of induction. This further confirmed that apoptosis is a major cause of cell death.

Apoptosis includes caspase-dependent apoptosis and caspase-independent apoptosis (Liu et al., 2013). In caspase-dependent apoptosis, the caspase family is a key mediator of cell death. As the preferred method for detecting apoptosis (Zhou et al., 2012), transmission electron microscopy plays a crucial role in its detection (Ji et al., 2011; Würstle et al., 2012). Our findings revealed that caspase-dependent apoptosis is a major apoptotic pathway during cell differentiation. Furthermore, the numbers of caspase-9- and caspase-3-positive cells increased over time and were associated with apoptosis of astrocytes differentiated from adipose-derived stromal cells. The expression rate of caspase-9, the main initiation factor of apoptosis (Fombonne et al., 2012; White et al., 2012; Brentnall et al., 2013; Qin et al., 2013), reached 30.27% at 21 days of induction. However, for caspase-3, the rate was 46.47%, significantly higher than that for caspase-9, suggesting a significant amplification effect. For both caspase-3 and caspase-9, expression is mainly in the cytoplasm, especially around the nucleus; however, there is no significant expression in the protrusions of the induced cells. The expression of caspase-9 was less than the expression of executioner caspase-3, suggesting an amplification effect in the process of induction.

During the differentiation of adipose-derived stromal cells into astrocytes, expression of glial fibrillary acidic protein, an important marker of astrocytes (Bernal and Peterson, 2011; Sokolowski et al., 2011; Yeh et al., 2011; Sukumari-Ramesh et al., 2012; Hoppe et al., 2013), is evenly detected in the cytoplasm as well as in the protrusions. Glial fibrillary acidic protein bundles are evenly distributed in the cytoplasm as well as in the cell processes of normal astrocytes differentiated from adipose-derived stromal cells. More organelles are observed, including mitochondria, endoplasmic reticulum and lysosomes. There is more euchromatin and less heterochromatin in nuclei, and the heterochromatin is dispersed. In contrast, in the cytoplasm of apoptotic cells, the mitochondria, concentrated around the nuclei, were significantly swollen, the cristae were ruptured, and vacuolization was observed. The membranes of nuclei were wrinkled, and some were fragmented. The chromatin was condensed and distributed at the membrane, with a block or crescent shape, typical of apoptosis. Finally, cell morphological changes, including shrinkage, and a decrease or even disappearance of protrusions and microvilli occur.

In summary, adipose-derived stromal cells can differentiate into astrocytes using a chemical inducer mainly consisting of 3-isobutyl-1-methylxanthine. The number of living cells decreases over the duration of induction. Caspase-dependent apoptosis is the main pathway of apoptosis during induction.

**Author contributions:** *Yuan XD was responsible for writing the manuscript, study design, concept, implementation and data arrangement. Sun QY, Ou Y and Zhang LL performed the whole*
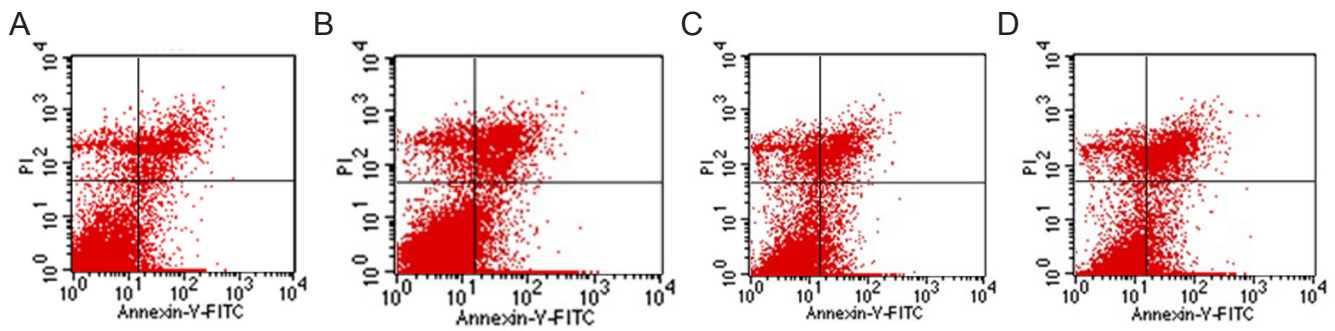
**Figure 5 Quantitative distribution of early apoptosis of Adipose-derived stromal cells at various time points after differentiation, as detected by flow cytometry.**

(A) At 48 hours, values in the upper left quadrant, upper right quadrant, lower left quadrant and lower right quadrant were 3.55%, 8.55%, 83.29% and 4.62%, respectively. (B) At 7 days, values in the upper left quadrant, upper right quadrant, lower left quadrant and lower right quadrant were 4.39%, 10.79%, 77.08% and 7.74%, respectively. (C) At 14 days, values in the upper left quadrant, upper right quadrant, lower left quadrant and lower right quadrant were 6.65%, 8.66%, 72.69% and 12.01%, respectively. (D) At 21 days, values in the upper left quadrant, upper right quadrant, lower left quadrant and lower right quadrant were 4.98%, 10.85%, 69.86% and 14.32%, respectively. The upper left quadrant: Annexin $V^-PI^+$ representing mechanically damaged cells. The upper right quadrant: Annexin $V^+PI^+$ representing late apoptotic or necrotic cells. Lower left quadrant: Annexin $V^-PI^-$ representing living cells. Lower right quadrant: Annexin $V^+PI^-$ representing early apoptotic cells.
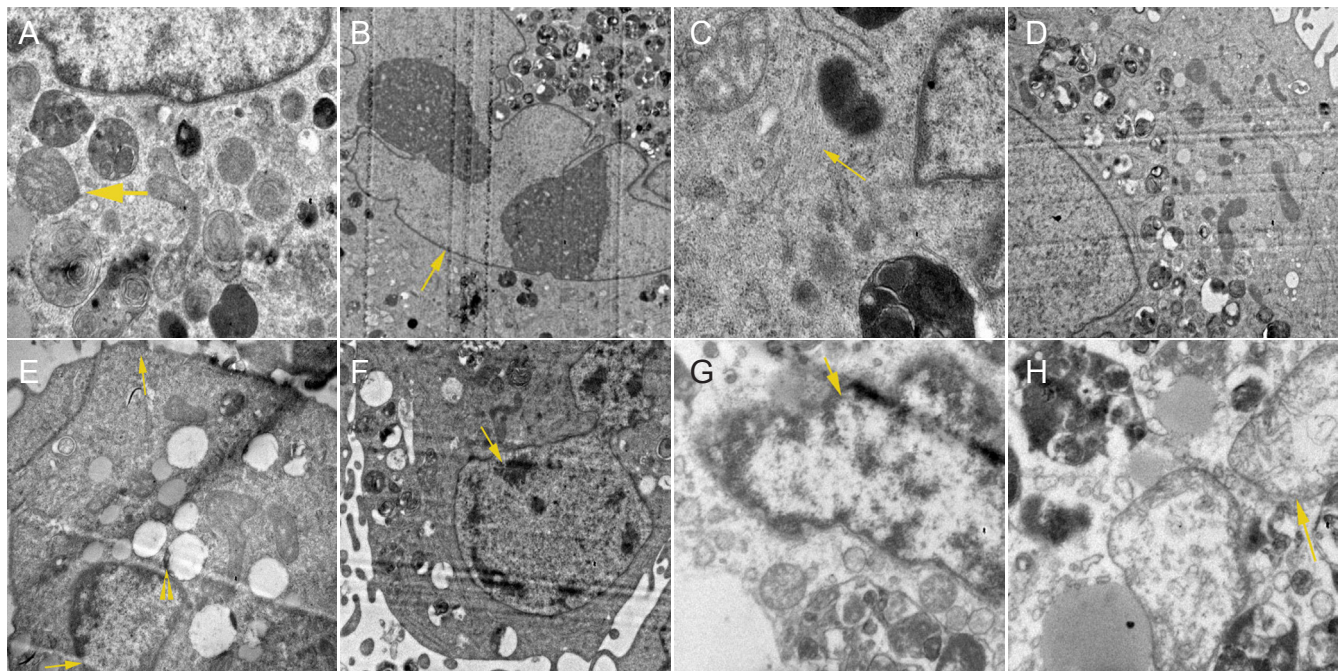


**Figure 6 Ultrastructural characteristics of adipose-derived stromal cells-differentiated astrocytes and apoptotic cells at 14 days (transmission electron microscopy).**

(A–D) Mitochondria (A, arrow, × 15,000), nucleoli (B, arrow, × 7,000), glial fibers (C, arrow, × 30,000) and protuberances (D, arrow, × 5,000) of astrocytes differentiated from Adipose-derived stromal cells appear normal. (E–G) Ultrastructure of apoptotic cells. Microvilli (arrows) on the membrane surface disappeared, resulting in a smooth appearance, the chromatin was crescent-shaped, and mitochondrial vacuolar degeneration was present (E, × 15,000). Chromatin (arrow) was blocky and condensed (F, × 10,000). Nuclear condensation was present (G, × 15,000), the mitochondria were swollen, and cristae were ruptured (H, × 15,000).

## References

Adrain C, Creagh EM, Martin SJ (2001) Apoptosis-associated release of Smac/DIABLO from mitochondria requires active caspases and is blocked by Bcl-2. EMBO J 20:6627-6636.

Ashjian PH, Elbarbary AS, Edmonds B, DeUgarte D, Zhu M, Zuk PA, Lorenz HP, Benhaim P, Hedrick MH (2003) In vitro differentiation of human processed lipoaspirate cells into early neural progenitors. Plast Reconstr Surg 111:1922-1931.

Bernal GM, Peterson DA (2011) Phenotypic and gene expression modification with normal brain aging in GFAP-positive astrocytes and neural stem cells. Aging cell 10:466-482.

Brentnall M, Rodriguez-Menacol L, De Guevara RL, Cepero E, Boise LH (2013) Caspase-9, caspase-3 and caspase-7 have distinct roles during intrinsic apoptosis. BMC Cell Biol 14:32.

Cai YN, Yuan XD, Ou Y, Lu YH (2011) Apoptosis during β-mercaptoethanol-induced differentiation of adult adipose-derived stromal cells into neurons. Neural Regen Res 6:750-755.

Chen M, Wang J (2002) Initiator caspases in apoptosis signaling pathways. Apoptosis 7:313-319.

Compton MM, Cidlowski JA (1986) Rapid in vivo effects of glucocorticoids on the integrity of rat lymphocyte genomic deoxyribonucleic acid. Endocrinology 118:38-45.

Daniel P (2000) Dissecting the pathways to death. Leukemia 14:2035-2044.

Di Giorgio FP, Carrasco MA, Siao MC, Maniatis T, Eggan K (2007) Non-cell autonomous effect of glia on motor neurons in an embryonic stem cell-based ALS model. Nat Neurosci 10:608-614.

Fombonne J, Bissey PA, Guix C, Sadoul R, Thibert C, Mehlen P (2012) Patched dependence receptor triggers apoptosis through ubiquitination of caspase-9. Proc Natl Acad Sci U S A 109:10510-10515.

Freire MA (2012) Pathophysiology of neurodegeneration following traumatic brain injury. West Indian Med J 61:751-755.

Giansanti V, Torriglia A, Scovassi AI (2011) Conversation between apoptosis and autophagy:"is it your turn or mine?". Apoptosis 16: 321-333.

Gil J, Esteban M (2000) Induction of apoptosis by the dsRNA-dependent protein kinase (PKR): mechanism of action. Apoptosis 5:107-114.

Goldman S (2005) Stem and progenitor cell–based therapy of the human central nervous system. Nat Biotechnol 23:862-871.

Grebeňová D, Kuželová K, Fuchs O, Halada P, Havlíček V, Marinov I, Hrkal Z (2004) Interferon-alpha suppresses proliferation of chronic myelogenous leukemia cells K562 by extending cell cycle S-phase without inducing apoptosis. Blood Cells Mol Dis 32:262-269.

Guo FH, Chen DM, Liu Z, Wen K, Du J (2011) Progress of apoptosis imaging using Annexin V labeled with positron radionuclides. Yuanzineng Kexue Jishu 45:908-914.

Holden C (2007) Neuroscience. Astrocytes secrete substance that kills motor neurons in ALS. Science 316:353.

Hoppe JB, Rattray M, Tu H, Salbego CG, Cimarosti H (2013) SUMO-1 conjugation blocks beta-amyloid-induced astrocyte reactivity. Neurosci Lett 546:51-56.

Igder S, Asadikaram GR, Sheykholeslam F, Sayadi AR, Mahmoodi M, Kazemi Arababadi M, Rasaee MJ (2013) Opium induces apoptosis in Jurkat cells. Addict Health 5:27-34.

Jacobsen JS, Wu CC, Redwine JM, Comery TA, Arias R, Bowlby M, Martone R, Morrison JH, Pangalos MN, Reinhart PH, Bloom FE (2006) Early-onset behavioral and synaptic deficits in a mouse model of Alzheimer's disease. Proc Natl Acad Sci U S A 103:5161-5166.

Ji YB, Qu ZY, Zou X (2011) Juglone-induced apoptosis in human gastric cancer SGC-7901 cells via the mitochondrial pathway. Exp Toxicol Pathol 63:69-78.

Johansson AC, Appelqvist H, Nilsson C, Kågedal K, Roberg K, Öllinger K (2010) Regulation of apoptosis-associated lysosomal membrane permeabilization. Apoptosis 15:527-540.

Kang JW, Kim JH, Song K, Kim SH, Yoon JH, Kim KS (2010) Kaempferol and quercetin, components of Ginkgo biloba extract (EGb 761), induce caspase-3-dependent apoptosis in oral cavity cancer cells. Phytother Res 24:S77-82.

Kang SK, Lee DH, Bae YC, Kim HK, Baik SY, Jung JS (2003) Improvement of neurological deficits by intracerebral transplantation of human adipose tissue-derived stromal cells after cerebral ischemia in rats. Exp Neurol 183:355-366.

Kavitha K, Vidya Priyadarsini R, Anitha P, Ramalingam K, Sakthivel R, Purushothaman G, Singh AK, Karunagaran D, Nagini S (2012) Nimbolide, a neem limonoid abrogates canonical NF-κB and Wnt signaling to induce caspase-dependent apoptosis in human hepatocarcinoma (HepG2) cells. Eur J Pharmacol 681:6-14.

Liu TM, Martina M, Hutmacher DW, Hui JHP, Lee EH, Lim B (2007) Identification of common pathways mediating differentiation of bone marrow-and adipose tissue-derived human mesenchymal stem cells into three mesenchymal lineages. Stem Cells 25:750-760.

Liu YH, Yuan XD, Ye CQ, Ou Y, Cai YN (2010) Adult adipose-derived stem cells differentiation into a satrocyte cells morphology and ultrastructure in vitro. Zhonghua Xingwei Kexue yu Nao Kexue Zazhi 19: 617-620.

Lu YH, Yuan XD, Ou Y, Cai YN, Wang SJ, Sun QY, Zhang WL (2012) Autophagy and apoptosis during adult adipose-derived stromal cells differentiation into neuron-like cells in vitro. Neural Regen Res 7:1205-1212.

McIntosh K, Zvonic S, Garrett S, Mitchell JB, Floyd ZE, Hammill L, Kloster A, Di Halvorsen Y, Ting JP, Storms RW, Goh B, Kilroy G, Wu X, Gimble JM (2006) The immunogenicity of human adipose-derived cells: temporal changes in vitro. Stem Cells 24:1246-1253.

Nakagami H, Morishita R, Maeda K, Kikuchi Y, Ogihara T, Kaneda Y (2006) Adipose tissue-derived stromal cells as a novel option for regenerative cell therapy. J Atheroscler Thromb 13:77.

Nicoletti I, Migliorati G, Pagliacci M, Grignani F, Riccardi C (1991) A rapid and simple method for measuring thymocyte apoptosis by propidium iodide staining and flow cytometry. J Immunol Methods 139:271-279.

Ou Y, Yuan XD, Cai YN, Lu YH (2011a) Ultrastructure and electrophysiology of astrocytes differentiated from adult adipose-derived stromal cells. Chin Med J (Engl) 124:2656-2660.

Ou Y, Yuan XD, Cai YN, Lu YH (2011b) A novel ethanol-based method to induce differentiation of adipose-derived stromal cells into astrocytes. Neural Regen Res 6:738-743.

Pekny M, Nilsson M (2005) Astrocyte activation and reactive gliosis. Glia 50:427-434.

Qin S, Yang C, Wang X, Xu C, Li S, Zhang B, Ren H (2013) Overexpression of Smac promotes cisplatin-induced apoptosis by activating caspase-3 and caspase-9 in lung cancer A549 cells. Cancer Biother Radiopharm 28:177-182.

Ren SX, Cheng AS, To KF, Tong JH, Li MS, Shen J, Wong CC, Zhang L, Chan RL, Wang XJ, Ng SS, Chiu LC, Marquez VE, Gallo RL, Chan FK, Yu J, Sung JJ, Wu WK, Cho CH (2012) Host immune defense peptide LL-37 activates caspase-independent apoptosis and suppresses colon cancer. Cancer Res 72:6512-6523.

Safford KM, Hicok KC, Safford SD, Halvorsen Y-DC, Wilkison WO, Gimble JM, Rice HE (2002) Neurogenic differentiation of murine and human adipose-derived stromal cells. Biochem Biophys Res Commun 294:371-379.

Samsel L, Zaidel G, Drumgoole HM, Jelovac D, Drachenberg C, Rhee JG, Brodie AM, Bielawska A, Smyth MJ (2004) The ceramide analog, B13, induces apoptosis in prostate cancer cell lines and inhibits tumor growth in prostate cancer xenografts. Prostate 58:382-393.

Slee EA, Adrain C, Martin SJ (2001) Executioner caspase-3, -6, and -7 perform distinct, non-redundant roles during the demolition phase of apoptosis. J Biol Chem 276:7320-7326.

Sokolowski JD, Nobles SL, Heffron DS, Park D, Ravichandran KS, Mandell JW (2011) Brain-specific angiogenesis inhibitor-1 expression in astrocytes and neurons: implications for its dual function as an apoptotic engulfment receptor. Brain Behav Immun 25:915-921.

Suárez L, Vidriales M-B, García-Laraña J, Sanz G, Moreno M-J, López A, Barrena S, Martínez R, Tormo M, Palomera L, Lavilla E, López-Berges MC, de Santiago M, de Equiza ME, Miguel JF, Orfao A (2004) CD34+ cells from acute myeloid leukemia, myelodysplastic syndromes, and normal bone marrow display different apoptosis and drug resistance-associated phenotypes. Clin Cancer Res 10:7599-7606.

Sukumari-Ramesh S, Alleyne CH, Dhandapani KM (2012) Astrocyte-specific expression of survivin after intracerebral hemorrhage in mice: a possible role in reactive gliosis? J Neurotrauma 29:2798-2804.

Tatsuta T, Hosono M, Sugawara S, Kariya Y, Ogawa Y, Hakomori S, Nitta K (2013) Sialic acid-binding lectin (leczyme) induces caspase-dependent apoptosis-mediated mitochondrial perturbation in Jurkat cells. Int J Oncol 43:1402.

Tognon R, Nunes ND, Castro FA (2013) Apoptosis deregulation in myeloproliferative neoplasms. Einstein (Sao Paulo) 11:540-544.

Van Den Bosch L, Robberecht W (2008) Crosstalk between astrocytes and motor neurons: what is the message? Exp Neurol 211:1-6.

Vittar NB, Awruch J, Azizuddin K, Rivarola V (2010) Caspase-independent apoptosis, in human MCF-7c3 breast cancer cells, following photodynamic therapy, with a novel water-soluble phthalocyanine. Int J Biochem Cell Biol 42:1123-1131.

von Roretz C, Lian XJ, Macri AM, Punjani N, Clair E, Drouin O, Dormoy-Raclet V, Ma JF, Gallouzi IE (2013) Apoptotic-induced cleavage shifts HuR from being a promoter of survival to an activator of caspase-mediated apoptosis. Cell Death Differ 20:154-168.

Würstle ML, Laussmann MA, Rehm M (2012) The central role of initiator caspase-9 in apoptosis signal transduction and the regulation of its activation and activity on the apoptosome. Exp Cell Res 318:1213-1220.

White MJ, Schoenwaelder SM, Josefsson EC, Jarman KE, Henley KJ, James C, Debrincat MA, Jackson SP, Huang DC, Kile BT (2012) Caspase-9 mediates the apoptotic death of megakaryocytes and platelets, but is dispensable for their generation and function. Blood 119:4283-4290.

Wirawan E, Walle LV, Kersse K, Cornelis S, Claerhout S, Vanoverberghe I, Roelandt R, De Rycke R, Verspurten J, Declercq W, Agostinis P, Vanden Berghe T, Lippens S, Vandenabeele P (2010) Caspase-mediated cleavage of Beclin-1 inactivates Beclin-1-induced autophagy and enhances apoptosis by promoting the release of proapoptotic factors from mitochondria. Cell Death Dis 1:e18.

Wlodkowic D, Skommer J, Akagi J, Fujimura Y, Takeda K (2013) Multi-parameter analysis of apoptosis using lab-on-a-chip flow cytometry. Curr Protoc Cytom 66:9.42.41-49.42.15.

Wyllie A (1980) Glucocorticoid-induced thymocyte apoptosis is associated with endogenous endonuclease activation. Nature 284:555-556.

Ye CQ, Yuan XD, Liu H, Cai YN, Ou Y (2010) Ultrastructure of neuronal-like cells differentiated from adult adipose-derived stromal cells. Neural Regen Res 5:1456-1463.

Yeh CY, Vadhwana B, Verkhratsky A, Rodriguez JJ (2011) Early astrocytic atrophy in the entorhinal cortex of a triple transgenic animal model of Alzheimer's disease. ASN Neuro 3:271-279.

Yoshimura H, Muneta T, Nimura A, Yokoyama A, Koga H, Sekiya I (2007) Comparison of rat mesenchymal stem cells derived from bone marrow, synovium, periosteum, adipose tissue, and muscle. Cell Tissue Res 327:449-462.

Zhang N, Chen Y, Jiang R, Li E, Chen X, Xi Z, Guo Y, Liu X, Zhou Y, Che Y, Jiang X (2011) PARP and RIP 1 are required for autophagy induced by 11′-deoxyverticillin A, which precedes caspase-dependent apoptosis. Autophagy 7:598-612.

Zhou A, Wang H, Lan K, Zhang X, Xu W, Yin Y, Li D, Yuan J, He Y (2012) Apoptosis induced by pneumolysin in human endothelial cells involves mitogen-activated protein kinase phosphorylation. Int J Mol Med 29:1025-1030.

Zuk PA, Zhu M, Mizuno H, Huang J, Futrell JW, Katz AJ, Benhaim P, Lorenz HP, Hedrick MH (2001) Multilineage cells from human adipose tissue: implications for cell-based therapies. Tissue Eng 7:211-228.

Zuk PA, Zhu M, Ashjian P, De Ugarte DA, Huang JI, Mizuno H, Alfonso ZC, Fraser JK, Benhaim P, Hedrick MH (2002) Human adipose tissue is a source of multipotent stem cells. Mol Biol Cell 13:4279-4295.

*Copyedited by Patel B, Frenchman B, Yu J, Qiu Y, Li CH, Song LP, Zhao M*